Multiconfiguration Dirac-Hartree-Fock energy levels and transition probabilities for W XXXVIII

Charlotte Froese Fischer
National Institute of Standards and Technology, Gaithersburg, Maryland 20899, USA

Gediminas Gaigalas*
Vilnius University, Institute of Theoretical Physics and Astronomy and A. Goštauto 12, LT-01108, Vilnius, Lithuania

(Received 10 January 2012; published 3 April 2012)

Energies, lifetimes, and wave-function compositions have been computed for all levels of $4p^6 4d$, $4p^6 4f$, and $4p^5 4d^2$ using single and double excitations from a multireference set (SD-MR) to generate expansions for the multiconfiguration Dirac-Hartree-Fock (MCDHF) approximation. An extended version of the general relativistic atomic structure package, GRASP2K, was used to deal with configuration state functions with as many as six open shells and with configurations containing as many as three f electrons. $E1$, $E2$, $M1$ transition probabilities are reported for transitions between the levels as supplemental material. Results are compared with other theory and with experiment, when available.

DOI: 10.1103/PhysRevA.85.042501 PACS number(s): 31.15.ag, 31.15.aj, 31.15.am

I. INTRODUCTION

Tungsten (W) is of great interest as a plasma wall material in the development of future tokamaks. Needed are atomic data for highly ionized tungsten atoms that may appear as impurities in hot plasmas. The feasibility of accurate theoretical studies for complex atoms with open f shells was investigated recently by Gaigalas *et al.* [1] and applied to W^{+24}. Without experimental data, the accuracy of transition data could only be related to the gauge dependence of the theoretical results.

Prominent lines in electron-beam ion-trap (EBIT) spectra of Rb-like W^{+37} to Cu-like W^{+45} ions have been measured for wavelengths and intensities by Utter *et al.* [2]. In their paper the identification of lines depended on theoretical predictions of wavelengths from *ab initio* calculations performed by Fournier [3] using a fully relativistic parametric potential code [4,5]. Quantum electrodynamic (QED) corrections were not included.

With some experimental data now available, the Rb-like spectrum of W^{+37} is an excellent test case for theory. The $4p^6 4d$ ground state and 10 excited levels of the $4p^6 4f$ and $4p^5 4d^2$ configurations that can be reached through electric dipole ($E1$) transitions from the ground configuration have been classified by Kramida and Shirai [6] from available observed wavelengths [7] through a least-squares process developed by Cowan [8]. Thus some energy levels and their uncertainty are accurately known. All configurations are part of the $n = 4$ complex with unfilled $4d$ and $4f$ subshells and there are strong interactions within this complex. Fournier [3] included a small set of configurations in his wave-function expansion with very few from the $n = 4$ complex. Bogdanovich *et al.* [9] applied a quasirelativistic (QR) method that included an algorithm for deciding on the important correlation corrections to these levels of W^{+37} and reported their lifetimes. Not included were other quantum electrodynamic (QED) corrections.

In the present paper we report all the energy levels of the even parity $4p^6 4d$ ground configuration as well as the $4p^5 4d^2$ and $4p^6 4f$ odd parity excited configurations. Transition probabilities ($E1$, $E2$, $M1$) for transitions between these levels are also reported. Accuracy is estimated by comparing the computed energy levels with those derived from observation and the agreement of length and velocity line strengths for $E1$ and $E2$ transition probabilities. The calculations were performed using a version of the general relativistic atomic structure package, GRASP2K [10]. In a revised version [11], the calculations of the spin-angular parts of matrix elements relied on a second quantization method in coupled tensorial form and quasispin technique [12,13]. This revision not only overcame some limitations on the complexity of the cases that could be executed successfully by GRASP2K but also increased the efficiency and the speed of angular integrations.

II. METHOD OF CALCULATIONS

The GRASP2K computer package and its revision are based on the multiconfiguration Dirac-Hartree-Fock (MCDHF) approach taking into account relativistic and QED corrections [13–15].

In this approach, an atomic state function (ASF) of parity P and total angular momentum J, $\Psi(\gamma PJ)$, is given by a linear combination of configuration state functions (CSFs) with the same parity, $\Phi(\gamma_i PJ)$, that is,

$$\Psi(\gamma PJ) = \sum_i c_i \Phi(\gamma_i PJ). \tag{1}$$

The multiconfiguration energy functional is based on the Dirac-Coulomb Hamiltonian, namely (in a.u.),

$$H_{\rm DC} = \sum_{j=1}^{N} [c\boldsymbol{\alpha}_j \boldsymbol{p}_j + (\beta_j - 1)c^2 + V(r_j)] + \sum_{j<k} \frac{1}{r_{jk}}, \tag{2}$$

where $\boldsymbol{\alpha}$ and β are 4×4 Dirac matrices, $\mathbf{p}$ is the momentum operator, $V(r_j)$ and $1/r_{jk}$ are the electrostatic electron-nucleus and electron-electron interactions, respectively. In all the calculations reported here, the nuclear charge distribution was modeled by the two-component Fermi function. A variational method was used to optimize the large and small components

*Gediminas.Gaigalas@tfai.vu.lt

TABLE I. Summary of the extended optimal level MCDHF calculations performed indicating the range of eigenvalues and the size of the interaction matrix for each J of the group.

J	Parity	Eigenvalues	Size
3/2, 5/2	+	1,1	17 538, 27 462
1/2, 3/2	−	1–7, 1–11	40 963, 82 461
5/2, 7/2	−	1–12, 1–10	111 273, 111 868
9/2, 11/2	−	1–5, 1–2	78 363, 41 334

of the radial functions that define the CSFs and their expansion coefficients in the wave function.

In the present case, there may be several CSFs that are important components to the wave-function expansion, defined in terms of orbitals with principal quantum number $n \leqslant 4$. These CSFs define a multireference set (MR). The most important corrections to the wave function arise from single and double excitations (SD) from orbitals occupied in the MR set to unfilled subshells. Because W^{+37} is so highly ionized, the most important contributions are CSFs within the $n = 4$ complex that interact with one or more members of the MR set. Included in the complex are CSFs with singly occupied or even unoccupied $4s$ subshells. Thus the excitation process needs to include excitations from the $4s^2$ subshell. The Ni-like $1s^2 \ldots 3d^{10}$ core was treated as an inactive core. When the SD excitations are restricted to $n = 4$ orbitals, we shall refer to the calculation as an $n = 4$ active set (AS) calculation. When the maximum principal quantum number is extended to $n = 5$ and $n = 6$, further corrections are included and the expansions increase in size significantly. Because the $4p^6 4f$ and $4p^5 4d^2$ CSFs only interact for $J = 5/2$ or $7/2$, optimization was done in groups as reported recently for Mo VI [16], namely: (i) $J = 1/2, 3/2$; (ii) $J = 5/2, 7/2$; (iii) $J = 9/2, 11/2$. In this extended optimal level (EOL) calculation, the same radial functions are used in the wave-function expansion for all levels of the group.

As a final step, a relativistic configuration interaction (RCI) calculation was performed to include the transverse-photon (Breit) interaction describing the transversely polarized photon contribution to the electron-electron interactions in the Coulomb gauge, the vacuum polarization (VP), and the self-energy (SE) corrections. Because the decrease in energy in going from $n = 4$ to $n = 5$ calculations was found to be rather small and contributions from $n = 6$ were expected to be even smaller, the rather large $n = 6$ expansions for odd parity were condensed to eliminate CSFs with an expansion coefficient less than 0.00001 from the Dirac-Coulomb (DC) wave functions. Table I summarizes the calculations performed for the four groups of levels by showing the J values and parity of each group, the levels that were included in the optimization process, and the size of the wave-function expansion for the $n = 6$ results reported as the final results for this paper.

Table II shows the contributions to the excitation energy arising from different parts of the Hamiltonian for several levels. As expected, the DC contribution is the largest, with the Breit (TP) interaction giving a significant correction. The vacuum polarization and self-energy corrections are of lesser importance. The DC contribution changes the most as the orbital set is expanded. Other corrections vary by lesser amounts. The effect of triple and quadruple excitations (TQ) from the reference set were neglected in this study. The total sum of these contributions is compared with experimental energy level [19]. These were derived from observed wavelengths by a least-squares fitting process that predicts energy levels and their uncertainties [6]. Table II also reports the difference between and the experimental and the computed energy levels (Total). In all cases, the difference is larger in magnitude than the uncertainty in the energy level and, in most cases, decreases as larger orbital sets are used in the expansion.

In Table III we present the computed energy levels and their lifetimes, along with the composition of the wave function in jj as well as LSJ coupling.

Tables IV and V report electric dipole ($E1$) transitions from the $^2D_{3/2}$ and $^2D_{5/2}$ levels, respectively, to the odd levels.

A similar table for the numerous $E2$ and $M1$ transitions between the odd parity levels is included with this paper as Supplemental Material [17].

III. COUPLINGS AND WAVE-FUNCTION COMPOSITION

The MCDHF calculations were performed with the wave function expanded in a basis of CSFs defined in terms of orbitals that are coupled in jj coupling. Usually results are presented in LSJ notation. In fact, the MCHF-MCDHF database [18] is designed only for this notation. If we make the assumption that the nl_- and nl MCDHF radial functions are the same, it is possible to transform the wave function from the jj-coupling scheme to LSJ coupling. The revised GRASP2K contains a program, JJ2LS, that rapidly transforms 99% of the wave-function composition of a large expansion to LSJ: A complete transformation is also possible but may take considerably more computer time. The contribution of a CSF to the composition is the square of the expansion coefficient in an orthonormal basis. Table III shows the larger contributions of the 49 levels considered in this paper in both jj and LSJ coupling.

In Table III, the jj-coupling notation of a CSF denotes the total J for a multiply occupied shell in parentheses, whereas the resultant of coupling two subshells or, in general, a subconfiguration and a subshell, is given in square brackets. The orbital $4d_-$, for example, is a $4d_{3/2}$ orbital whereas $4d$ is $4d_{5/2}$. In the LSJ notation, for brevity, CSFs for the $4p^5 4d^2$ configuration are denoted only by the LS term and seniority of the $4d^2$ subshell and the final LS term. Only in one case is the largest component of the wave function significantly greater in LSJ rather than in jj, namely, for the $4p^5 4s^2 (_2{}^3F)^4G^o$ $J = 9/2$ level at 1 382 620 cm^{-1} where the largest component in jj is 50% whereas the largest in LSJ is 70%. In others they are similar or LSJ is considerably less. Fournier [3] designated labels simply by the occupation of the different subshells in jj coupling. Without the intermediate quantum numbers such a designation is not always unique.

A wave function or a corresponding energy level is often designated as the label of the CSF with the largest expansion coefficient. As shown in the case of Mo VI [16], labels determined in this manner may not be unique. An algorithm has been proposed for defining unique labels. Basically, for a given set of wave functions for the same J and parity, the CSF with largest expansion coefficient is used as the label

TABLE II. Dirac-Coulomb (DC), transverse photon (TP), vacuum polarization (VP), and self-energy (SE) contributions to the energy (in cm^{-1}) as a function of the orbital set. The sum (Total) is compared with experiment and the difference (Diff.) is reported. All energies are relative to the ground state.

	DC	Breit (TP)	VP	SE	Total	Expt. [6,19]	Diff.
	(i) $4p^6 4d\ ^2D\ \ J = 5/2$						
$n = 4$	1 57 565.02	−3498.50	0.60	237.28	154 304.45	1 54 640 ± 120	−340
$n = 5$	1 58 136.24	−3377.23	−1.56	236.91	154 994.36	1 54 640 ± 120	350
$n = 6$	1 57 502.42	−3384.70	−1.43	237.07	154 353.36	1 54 640 ± 120	−290
	(ii) $4p^5 4d^2(_2{}^3F)\ ^4D\ \ J = 3/2$						
$n = 4$	1 225 740.23	−2629.03	25.15	−1456.09	1 221 680.26	1 227 640 ± 210	−5960
$n = 5$	1 225 850.85	−2698.77	28.52	−1456.03	1 221 724.57	1 227 640 ± 210	−5920
$n = 6$	1 225 589.32	−2685.36	26.36	−1456.45	1 221 473.87	1 227 640 ± 210	−6170
	(iii) $4p^5 4d^2(_2{}^3F)\ ^4D\ \ J = 1/2$						
$n = 4$	1 226 132.50	−3044.01	25.43	−1437.62	1 221 676.30	1 227 640 ± 210	−5960
$n = 5$	1 226 557.12	−3099.04	28.66	−1437.66	1 222 049.08	1 227 640 ± 210	−5590
$n = 6$	1 226 380.29	−3091.54	26.51	−1438.11	1 221 877.15	1 227 640 ± 210	−5760
	(iv) $4p^5 4d^2(_2{}^1G)\ ^2F\ \ J = 5/2$						
$n = 4$	1 523 453.12	−6672.53	20.39	−855.28	1 515 945.70	1 508 470 ± 100	7480
$n = 5$	1 519 890.96	−6760.73	23.38	−849.68	1 512 303.93	1 508 470 ± 100	3830
$n = 6$	1 518 779.48	−6655.53	19.95	−850.99	1 511 292.91	1 508 470 ± 100	2820
	(v) $4p^5 4d^2(_2{}^3F)\ ^4F\ \ J = 3/2$						
$n = 4$	1 557 569.50	−6449.14	42.77	−1227.78	1 549 935.35	1 542 600 ± 500	7300
$n = 5$	1 556 800.29	−6473.29	43.23	−1227.15	1 549 143.08	1 542 600 ± 500	6500
$n = 6$	1 555 763.55	−6391.42	41.16	−1227.61	1 548 185.68	1 542 600 ± 500	5600
	(vi) $4p^5 4d^2(_2{}^3F)\ ^2D\ \ J = 5/2$						
$n = 4$	1 755 868.66	−9303.69	45.57	−950.21	1 745 660.33	1 731 460 ± 130	14 200
$n = 5$	1 751 747.88	−9201.11	45.46	−928.33	1 741 663.90	1 731 460 ± 130	10 200
$n = 6$	1 750 071.01	−9055.42	42.42	−924.32	1 740 133.69	1 731 460 ± 130	8670
	(vii) $4p^6 4f\ ^2F\ \ J = 5/2$						
$n = 4$	1 782 471.08	−8579.18	39.86	−400.93	1 773 530.83	1 758 100 ± 180	15 400
$n = 5$	1 775 341.78	−8688.25	43.08	−424.31	1 766 272.30	1 758 100 ± 180	8200
$n = 6$	1 773 419.84	−8560.95	38.57	−427.11	1 764 470.35	1 758 100 ± 180	6400
	(viii) $4p^6 4f\ ^2F\ \ J = 7/2$						
$n = 4$	1 797 776.71	−9776.58	25.23	−254.51	1 787 770.85	1 769 600 ± 500	18 200
$n = 5$	1 788 853.62	−9797.36	28.91	−267.50	1 778 817.67	1 769 600 ± 500	9200
$n = 6$	1 786 887.52	−9645.09	24.29	−267.98	1 776 998.74	1 769 600 ± 500	7400
	(ix) $4p^5 4d^2(_2{}^3F)\ ^4G\ \ J = 5/2$						
$n = 4$	2 036 806.50	−11 442.54	212.98	−875.65	2 024 701.29	2 014 500 ± 300	10 200
$n = 5$	2 032 712.91	−11 386.54	212.83	−879.36	2 020 659.84	2 014 500 ± 300	6200
$n = 6$	2 031 249.97	−11 305.08	211.07	−880.79	2 019 275.17	2 014 500 ± 300	4800
	(x) $4p^5 4d^2(_2{}^3F)\ ^2D\ \ J = 3/2$						
$n = 4$	2 213 377.53	−11 531.25	230.28	−964.93	2 201 111.63	2 184 310 ± 220	16 800
$n = 5$	2 212 133.39	−11 494.28	226.73	−963.92	2 199 901.92	2 184 310 ± 220	15 590
$n = 6$	2 210 115.18	−11 341.36	224.93	−963.84	2 198 034.91	2 184 310 ± 220	13 720
	(xi) $4p^5 4d^2(_2{}^1G)\ ^2F\ \ J = 7/2$						
$n = 4$	2 340 324.95	−15 454.28	233.54	−659.27	2 324 444.94	2 325 500 ± 500	−1100
$n = 5$	2 335 255.64	−15 349.49	229.57	−659.03	2 319 476.69	2 325 500 ± 500	−6000
$n = 6$	2 333 386.32	−15 233.26	227.53	−658.16	2 317 722.43	2 325 500 ± 500	−7800

for the function containing this largest component. Once a label is assigned, the corresponding CSF is removed from consideration in the determination of the next label [20]. The last remaining label for a wave function may be based on a contribution that is exceedingly small as seen for the level at 1 742 142 cm^{-1} labeled $4p^5 4d^2(_2{}^3P)\ ^2D_{3/2}$ in Table III. The Atomic Spectra Database (ASD) [19] reports the leading percentage of the wave-function composition from calculations using the Cowan code [6,8]. Comparing the composition in Table III with ASD, we note that the

TABLE III. MCDHF energies (in cm^{-1}), lifetimes (in s), and wave-function composition of levels in W XXXVIII.

Label	J	Pos	Level (cm^{-1})	Lifetimes (s)	Composition	
					jj coupling	LSJ coupling
$4p^6\ 4d\ ^2D$	3/2	1			**98** $4p_-^2 4p^4 4d_-$	**98**
	5/2	1	154 353	2.53×10^{-5}	**98** $4p_-^2 4p^4 4d$	**98**
$4p^5\ 4d^2(_2^3F)\ ^4D^o$	3/2	1	1 221 474	8.10×10^{-10}	**87** $4p_-^2 4p^3 4d_-^2(2)$	**42** + **23**$(_2^3P)^4D$
	1/2	1	1 221 877	2.54×10^{-10}	**87** $4p_-^2 4p^3 4d_-^2(2)$	**84** + **11**$(_2^1D)^2P$
	5/2	2	1 354 946	1.53×10^{-8}	**84** $4p_-^2 4p^3 4d_-[0]4d$	**33** + **22**$(_2^3P)^4P$ + **15**$(_2^3P)^4D$
	7/2	9	2 267 787	3.10×10^{-12}	**85** $4p_- 4p^4 4d^2(4)$	**45** + **31**$(_2^3F)^2F$ + **18**$(_2^3F)^4F$
$^4F^o$	5/2	1	1 249 069	3.91×10^{-10}	**93** $4p_-^2 4p^3 4d_-^2(2)$	**36** + **18**$(_2^1D)^2D$ + **12**$(_2^3F)^4G$ + **10**$(_2^3F)^4D$
	7/2	2	1 382 497	2.93×10^{-10}	**71** $4p_-^2 4p^3 4d_-[1]4d$	**35** + **26**$(_2^3P)^4D$ + **16**$(_2^3F)^4D$ + **10**$(_2^1D)^2F$
	3/2	5	1 548 186	2.16×10^{-12}	**59** $4p_-^2 4p^3 4d_-[3]4d$	**32** + **22**$(_2^3P)^2D$ + **12**$(_2^3F)^2D$
	9/2	3	1 576 287	1.19×10^{-5}	**92** $4p_-^2 4p^3 4d^2(4)$	**38** + **29**$(_2^1G)^2G$ + **18**$(_2^3F)^2G$ + **13**$(_2^1G)^2H$
$^2G^o$	7/2	1	1 264 378	1.95×10^{-8}	**97** $4p_-^2 4p^3 4d_-^2(2)$	**31** + **32**$(_2^3F)^4G$ + **22**$(_2^1D)^2F$
	9/2	5	2 310 262	1.34×10^{-7}	**95** $4p_- 4p^4 4d^2(4)$	**31** + **23**$(_2^1G)^2H$ + **17**$(_2^3F)^4G$
$4p^5\ 4d^2(_2^3P)\ ^4P^o$	3/2	2	1 318 542	5.74×10^{-9}	**82** $4p_-^2 4p^3 4d_-^2(0)$	**28** + **21**$(_0^1S)^2P$ + **16**$(_2^3P)^4D$
	5/2	3	1 401 387	4.31×10^{-10}	**57** $4p_-^2 4p^3 4d_-[1]4d$	**41** + **17**$(_2^3F)^2F$ + **15**$(_2^1G)^2F$
	1/2	5	2 142 248	2.87×10^{-11}	**95** $4p_- 4p^4 4d_-[2]4d$	**46** + **31**$(_2^3P)^2S$ + **20**$(_2^3P)^4D$
$4p^5\ 4d^2(_2^3F)\ ^4G^o$	9/2	1	1 382 620	2.96×10^{-5}	**50** $4p_-^2 4p^3 4d_-[3]4d$	**70** + **15**$(_2^3F)^2G$ + **13**$(_2^3F)^4F$
	11/2	2	1 540 951	2.25×10^{-5}	**93** $4p_-^2 4p^3 4d^2(4)$	**57** + **41**$(_2^1G)^2H$
	5/2	9	2 019 275	8.90×10^{-13}	**84** $4p_- 4p^4 4d_-^2(2)$	**39** + **28**$(_2^3F)^2F$ + **14**$(_2^1D)^2F$
	7/2	8	2 118 127	7.57×10^{-10}	**97** $4p_- 4p^4 4d_-[2]4d$	**46** + **19**$(_2^3F)^2G$ + **14**$(_2^3F)^4F$
$4p^5\ 4d^2(_2^1D)\ ^2D^o$	3/2	3	1 396 088	1.24×10^{-10}	**63** $4p_-^2 4p^3 4d_-[1]4d$	**13** + **40**$(_2^3F)^4D$ + **14**$(_2^3F)^2D$ + **11**$(_2^1D)^2P$
	5/2	6	1 553 672	1.68×10^{-9}	**65** $4p_-^2 4p^3 4d^2(2)$	**24** + **18**$(_2^3P)^4P$ + **15**$(_2^3F)^2D$ + **13**$(_2^3P)^2D$
$4p^5\ 4d^2(_2^1G)\ ^2H^o$	11/2	1	1 415 613	2.80×10^{-3}	**93** $4p_-^2 4p^3 4d_-[3]4d$	**57** + **41**$(_2^3F)^4G$
	9/2	4	2 162 095	1.44×10^{-7}	**95** $4p_- 4p^4 4d_-[2]4d$	**45** + **19**$(_2^1G)^2G$ + **16**$(_2^3F)^2G$ + **10**$(_2^3F)^4G$
$^2G^o$	7/2	3	1 419 324	3.58×10^{-6}	**77** $4p_-^2 4p^3 4d_-[3]4d$ +**17** $4p_-^2 4p^3 4d_-[2]4d$	**15** + **29**$(_2^3F)^2G$ + **15**$(_2^3F)^2F$ + **15**$(_2^3F)^4F$ +**14**$(_2^1G)^2F$ +**15**$(_2^3F)^4F$ + **11**$(_2^1G)^2G$
	9/2	2	1 474 980	1.51×10^{-4}	**47** $4p_-^2 4p^3 4d_-[3]4d$ +**46** $4p_-^2 4p^3 4d_-[2]4d$	**38** + **24**$(_2^3F)^4F$ + **18**$(_2^3F)^2G$ +**17**$(_2^1G)^2H$
$4p^5\ 4d^2(_2^3P)\ ^2S^o$	1/2	2	1 431 711	9.63×10^{-6}	**80** $4p_-^2 4p^3 4d_-[2]4d$	**29** + **33**$(_2^3P)^4P$ + **19**$(_2^1D)^2P$
$^4D^o$	7/2	4	1 453 386	5.09×10^{-8}	**59** $4p_-^2 4p^3 4d_-[2]4d$ +**20** $4p_-^2 4p^3 4d_-[3]4d$	**20** + **13**$(_2^1D)^2F$ + **13**$(_2^1G)^2G$ + **12**$(_2^1G)^2F$ +**11**$(_2^3F)^4D$
	5/2	4	1 458 234	1.46×10^{-10}	**55** $4p_-^2 4p^3 4d_-[3]4d$	**36** + **25**$(_2^3P)^2D$ + **14**$(_2^1D)^2D$
	3/2	8	2 134 981	1.02×10^{-11}	**94** $4p_- 4p^4 4d_-[2]4d$	**37** + **16**$(_2^3F)^2D$ + **10**$(_2^3P)^2D$ + **10**$(_2^3F)^4F$
	1/2	6	2 144 727	5.78×10^{-13}	**87** $4p_- 4p^4 4d_-^2(0)$	**37** + **34**$(_2^3P)^2P$ + **21**$(_0^1S)^2P$
$^4S^o$	3/2	4	1 465 969	3.31×10^{-9}	**60** $4p_-^2 4p^3 4d_-[2]4d$	**30** + **25**$(_2^3P)^2D$ + **17**$(_2^3P)^4P$
$4p^5\ 4d^2(_2^1G)\ ^2F^o$	5/2	5	1 511 293	6.00×10^{-12}	**39** $4p_-^2 4p^3 4d_-[2]4d$ +**27** $4p_-^2 4p^4 4f_-$ +**13** $4p_-^2 4p^3 4d_-[1]4d$	**41** + **27**$4p^6 4f\ ^2F$ + **13**$(_2^3F)^2F$
	7/2	10	2 317 722	5.26×10^{-13}	**79** $4p_- 4p^4 4d_-[1]4d$	**53** + **29**$(_2^1G)^2G$
$4p^5\ 4d^2(_2^1D)\ ^2F^o$	7/2	5	1 558 637	5.07×10^{-11}	**68** $4p_-^2 4p^3 4d^2(2)$	**33** + **29**$(_2^3P)^4D$ + $4p^6 4f\ ^2F$
	5/2	12	2 325 721	2.76×10^{-10}	**97** $4p_- 4p^4 4d^2(2)$	**35** + **24**$(_2^3P)^2D$ + **18**$(_2^3P)^4D$
$^2P^o$	1/2	3	1 587 523	5.26×10^{-12}	**74** $4p_-^2 4p^3 4d^2(2)$	**66** + **14**$(_2^3P)^4P$ + **10**$(_2^3P)^2S$
	3/2	10	2 304 542	5.73×10^{-12}	**90** $4p_- 4p^4 4d^2(2)$	**32** + **26**$(_2^1D)^2D$ + **12**$(_2^3P)^4P$ + **11**$(_2^3P)^4D$
$4p^5\ 4d^2(_2^3P)\ ^2P^o$	1/2	4	1 621 723	1.60×10^{-12}	**52** $4p_-^2 4p^3 4d_-[3]4d$	**52** + **23**$(_2^3P)^4D$ + **20**$(_2^3P)^2S$
	3/2	11	2 321 806	4.71×10^{-13}	**84** $4p_- 4p^4 4d_-[1]4d$	**52** + **19**$(_2^3P)^4S$ + **10**$(_2^3P)^4P$
$4p^5\ 4d^2(_2^3F)\ ^2F^o$	7/2	6	1 645 220	4.23×10^{-11}	**50** $4p_-^2 4p^3 4d^2(4)$ +**29** $4p_-^2 4p^3 4d^2(2)$	**17** + **16**$4p^6 4f\ ^2F$ + **15**$(_2^1D)^2F$ + **14**$(_2^3F)^4D$ +**12**$(_2^3P)^4D$ + **11**$(_2^1G)^2G$
	5/2	7	1 740 134	1.07×10^{-12}	**37** $4p_-^2 4p^3 4d^2(4)$ +**18** $4p_-^2 4p^3 4d^2(2)$ +**14** $4p_-^2 4p^3 4d_-[1]4d$	**4** + **30**$(_2^3F)^2D$ + **16**$(_2^3F)^4F$ + **10**$4p^6 4f\ ^2F$ +**10**$(_2^3F)^4D$ + **9**$(_2^1D)^2F$ + **5**$(_2^1D)^2D$ + **5**$(_2^3P)^4D$
$4p^5\ 4d^2(_0^1S)\ ^2P^o$	3/2	6	1 679 761	5.97×10^{-10}	**66** $4p_-^2 4p^3 4d^2(0)$	**50** + **14**$(_2^3P)^2D$ + **10**$(_2^3P)^4S$
	1/2	7	2 395 225	3.27×10^{-11}	**94** $4p_- 4p^4 4d^2(0)$	**75** + **13**$(_2^3P)^4D$
$4p^5\ 4d^2(_2^3P)\ ^2D^o$	3/2	7	1 742 142	1.58×10^{-12}	**58** $4p_-^2 4p^3 4d^2(2)$ +**26** $4p_-^2 4p^3 4d^2(0)$ +**6** $4p_-^2 4p^3 4d_-[1]4d$	**0.4** + **20**$(_0^1S)^2P$ + **17**$(_2^3P)^4S$ + **16**$(_2^3P)^2P$ +**13**$(_2^1D)^2D$ + **12**$(_2^3P)^4D$ + **8**$(_2^3P)^4P$ + **4**$(_2^3F)^4F$ + **0.5**$(_2^3F)^2D$
	5/2	10	2 125 762	1.72×10^{-11}	**95** $4p_- 4p^4 4d_-[2]4d$	**14** + **18**$(_2^3F)^4F$ + **16**$(_2^1D)^2F$ + **14**$(_2^3F)^4G$

TABLE III. (*Continued*).

Label	J	Pos	Level (cm^{-1})	Lifetimes (s)	Composition	
					jj coupling	LSJ coupling
						$+\mathbf{12}(_2^3F)^2D\ +\mathbf{10}(_2^3P)^4D$
$4p^6\ 4f\ ^2F^o$	5/2	8	1 764 470	1.21×10^{-12}	$\mathbf{53}\ 4p_-^2 4p^4 4f_-$	$\mathbf{53}\ +\mathbf{18}(_2^1G)^2F$
	7/2	7	1 776 999	1.75×10^{-12}	$\mathbf{64}\ 4p_-^2 4p^4 4f$	$\mathbf{33}\ +\mathbf{29}(_2^3P)^4D\ +\mathbf{13}4p^6 4f\ ^2F$
$4p^5\ 4d^2(_2^3F)\ ^2D^o$	3/2	9	2 198 035	3.11×10^{-13}	$\mathbf{87}\ 4p_-4p^4 4d_-^2(2)$	$\mathbf{44}\ +\mathbf{17}(_2^1D)^2D\ +\mathbf{12}(_2^3F)^4F$
	5/2	11	2 302 432	4.00×10^{-13}	$\mathbf{87}\ 4p_-4p^4 4d_-[1]4d$	$\mathbf{34}\ +\mathbf{12}(_2^3P)^2D\ +\mathbf{10}(_2^3F)^4D\ +\mathbf{10}(_2^3F)^4F$

ground state is only 98% $4p^6 4d$ in the present work whereas it accounts for 100% of the wave-function compositions in ASD. In the MCDHF expansion most of the remaining composition is accounted for by the configurations $4p^5 4d 4f$ and$4p^4 4d^3$, configurations not included in the calculations for the data given in ASD [6,19].

Table VI compares the present jj and LSJ compositions with ASD compositions, obtained from a least-squares fitting of observed wavelengths using the Cowan code [6], for three levels. In the first example, a major contribution is from $4p^6 4f$ and its composition is essentially the same in all cases. In the second, there appears to be agreement, but for the third, there is a difference in the coupling of the dominant component. One of the features of $4p^5 4d^2$ CSFs and their interaction matrix is that there are many different couplings for the same final J value. In fact, Table I indicates that there are 11 different couplings for $J = 3/2$. It is not clear that the two very different methods would yield the same composition. Whereas the present method is an *ab initio* method, the other is semiempirical. Table III includes an energy level that could be a contender for the $4p^5 4d^2(_2^1D)(1/2,2)$ label used in ASD, namely $4p^5 4d^2(_2^1D)\ ^2P_{3/2}$ with a computed energy of 2 304 542 cm^{-1}. However, the line with the largest measured intensity [2] was observed at 45.7810(22) Å and was classified as a 3/2–3/2 transition from the ground state to $4p_-4p^4 4d_-^2$. The wavelength for a transition from the ground state to the observed level at 2 184 310 cm^{-1} would be 45.7810 Å. According to Table IV for $E1$ transition probabilities, the upper level with the largest transition rate from the ground state is $4p^5 4d^2(_2^3F)\ ^2D_{3/2}$ with a computed wavelength of 45.495 Å, in excellent agreement with observation. Thus we believe there is a difference in the label with ASD as well as a difference in composition. Tables II and III are based on this assumption.

IV. COMPARISON WITH OTHER THEORY AND EXPERIMENT

For transition probability calculations the important accuracy indicators [21] are the accuracy of the transition energies and the agreement in the length and velocity forms of the line strength for electric multipole transitions.

Figure 1 compares quasirelativistic (QR) [9], parametric potential (PP) [3], and observed [6] energy levels relative to present values as a function of the computed energies. For plotting purposes, the position of the $4d\ ^2D_{5/2}$ level has been moved to an energy within the graph. The observed fine-structure splitting is somewhat larger than our computed value but the latter is in considerably better agreement with observed than the other theories. With the exception of the highest observed level, $4p^5 4d^2(_2^1G)\ ^2F_{7/2}$, all other levels from all theories are higher than observed, with present values being higher by less than 0.5%. In nearly all cases the present energies are in better agreement with ASD than QR results which, in turn, are considerably better than the earlier PP values. The latter did not include a sufficient number of configurations from the $n = 4$ complex, particularly the configurations that result from $4p^2 \rightarrow 4d^2$ excitation from CSFs in the multireference set. For higher levels, the PP values are too high by about 20 000 cm^{-1}. From the present work, the least accurate energy is for the $4p^5 4d^2(_2^3F)\ ^2D_{3/2}$ level for which there is a disagreement in the label with ASD. The present label agrees with the QR label [9].

Table VII compares PP [3] and present wavelengths for some observed wavelengths. Present results are a considerable improvement and are in error by $\leqslant 0.7\%$.

Another factor in the accuracy of a transition probability, A_{ki}, is the accuracy of the line strength. In Tables IV and V, δT represents the discrepancy in the length and velocity forms of the transition probability when observed transition energies or wavelengths are used. When transition energies are sufficiently accurate, this is equivalent to the discrepancy in the line strength, namely $|S_l - S_v|/\max(S_l, S_v)$. This accuracy indicator varies considerably from one transition to the next. In these tables the LSJ labels are used so that it is possible to identify transitions that are essentially "LS forbidden" with

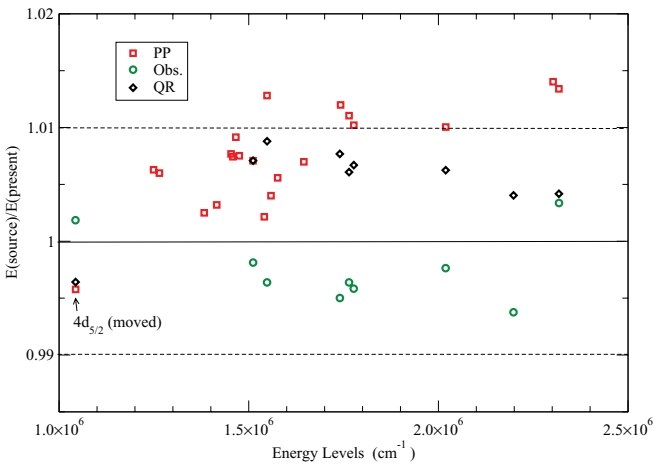

FIG. 1. (Color online) Comparison of quasirelativistic (QR) [9], parametric potential (PP) [3] energy levels with values derived from observation [6,19] as a function of the energy. The energy position of $4p^6 4d\ ^2D_{5/2}$ has been moved to a position on the graph.

TABLE IV. MCDHF transition data for $E1$ transitions from $4p^6 4d\ ^2D_{3/2}$: levels and $2J$ for lower level i, upper level k, wavelength λ (in Å), line strength S (length form), oscillator strength f (length form), transition rate A_{ki} (length form) in s^{-1}.

Levels		$2J$						
i	k	i	k	λ (Å)	S	f	A_{ki} (s^{-1})	δT
$4p^6 4d$	$- 4p^5 4d^2(^3F)$							
^2D	$^4D^o$	3	3	81.868	1.297×10^{-3}	4.811×10^{-3}	1.197×10^{9}	0.092
		3	1	81.841	2.130×10^{-3}	7.907×10^{-3}	3.937×10^{9}	0.095
^2D	$^4F^o$	3	5	80.060	3.532×10^{-3}	1.340×10^{-2}	2.324×10^{9}	0.052
$4p^6 4d$	$- 4p^5 4d^2(^3P)$							
^2D	$^4P^o$	3	3	75.841	1.149×10^{-5}	4.600×10^{-5}	1.334×10^{7}	0.508
$4p^6 4d$	$- 4p^5 4d^2(^3F)$							
^2D	$^4D^o$	3	5	73.804	7.725×10^{-5}	3.179×10^{-4}	6.489×10^{7}	0.135
$4p^6 4d$	$- 4p^5 4d^2(^1D)$							
^2D	$^2D^o$	3	3	71.629	4.476×10^{-3}	1.898×10^{-2}	6.169×10^{9}	0.028
$4p^6 4d$	$- 4p^5 4d^2(^3P)$							
^2D	$^4P^o$	3	5	71.358	2.804×10^{-5}	1.194×10^{-4}	2.606×10^{7}	0.218
^2D	$^2S^o$	3	1	69.847	2.239×10^{-8}	9.736×10^{-8}	6.656×10^{4}	0.950
^2D	$^4D^o$	3	5	68.576	6.544×10^{-3}	2.898×10^{-2}	6.852×10^{9}	0.001
^2D	$^4S^o$	3	3	68.214	5.901×10^{-5}	2.628×10^{-4}	9.417×10^{7}	0.179
$4p^6 4d$	$- 4p^5 4d^2(^1G)$							
^2D	$^2F^o$	3	5	66.169	1.428×10^{-1}	6.553×10^{-1}	1.664×10^{11}	0.004
$4p^6 4d$	$- 4p^5 4d^2(^3F)$							
^2D	$^4F^o$	3	3	64.592	2.455×10^{-1}	1.155	4.615×10^{11}	0.011
$4p^6 4d$	$- 4p^5 4d^2(^1D)$							
^2D	$^2D^o$	3	5	64.364	9.554×10^{-5}	4.509×10^{-4}	1.210×10^{8}	0.108
^2D	$^2P^o$	3	1	62.991	4.688×10^{-2}	2.260×10^{-1}	1.900×10^{11}	0.027
$4p^6 4d$	$- 4p^5 4d^2(^3P)$							
^2D	$^2P^o$	3	1	61.663	1.449×10^{-1}	7.139×10^{-1}	6.262×10^{11}	0.018
$4p^6 4d$	$- 4p^5 4d^2(^1S)$							
^2D	$^2P^o$	3	3	59.532	1.732×10^{-4}	8.839×10^{-4}	4.159×10^{8}	0.032
$4p^6 4d$	$- 4p^5 4d^2(^3F)$							
^2D	$^2F^o$	3	5	57.467	2.484×10^{-1}	1.313	4.420×10^{11}	0.012
$4p^6 4d$	$- 4p^5 4d^2(^3P)$							
^2D	$^2D^o$	3	3	57.401	7.383×10^{-5}	3.907×10^{-4}	1.977×10^{8}	0.267
$4p^6 4d$	$- 4p^6 4f$							
^2D	$^2F^o$	3	5	56.674	3.190×10^{-1}	1.710	5.918×10^{11}	0.013
$4p^6 4d$	$- 4p^5 4d^2(^3F)$							
^2D	$^4G^o$	3	5	49.523	4.039×10^{-1}	2.478	1.123×10^{12}	0.007
$4p^6 4d$	$- 4p^5 4d^2(^3P)$							
^2D	$^2D^o$	3	5	47.042	2.032×10^{-3}	1.312×10^{-2}	6.592×10^{9}	0.005
^2D	$^4D^o$	3	3	46.839	1.691×10^{-2}	1.096×10^{-1}	8.334×10^{10}	0.003
^2D	$^4P^o$	3	1	46.680	3.494×10^{-3}	2.274×10^{-2}	3.480×10^{10}	0.010
^2D	$^4D^o$	3	1	46.626	1.731×10^{-1}	1.128	1.730×10^{12}	0.010
$4p^6 4d$	$- 4p^5 4d^2(^3F)$							
^2D	$^2D^o$	3	3	45.495	5.950×10^{-1}	3.973	3.200×10^{12}	0.003
		3	5	43.432	1.379×10^{-4}	9.643×10^{-4}	5.683×10^{8}	0.030
$4p^6 4d$	$- 4p^5 4d^2(^1D)$							
^2D	$^2P^o$	3	3	43.393	2.460×10^{-3}	1.722×10^{-2}	1.525×10^{10}	0.007
$4p^6 4d$	$- 4p^5 4d^2(^3P)$							
^2D	$^2P^o$	3	3	43.070	5.718×10^{-4}	4.032×10^{-3}	3.625×10^{9}	0.056
$4p^6 4d$	$- 4p^5 4d^2(^1D)$							
^2D	$^2F^o$	3	5	42.997	7.497×10^{-6}	5.297×10^{-5}	3.185×10^{7}	0.002
$4p^6 4d$	$- 4p^5 4d^2(^1S)$							
^2D	$^2P^o$	3	1	41.750	2.193×10^{-3}	1.596×10^{-2}	3.053×10^{10}	0.009

TABLE V. MCDHF transition data for $E1$ transitions from $4p^6 4d\ ^2D_{5/2}$: levels and $2J$ for lower level i, upper level k, wavelength λ (in Å), line strength S (length form), oscillator strength f (length form), transition rate A_{ki} (length form) in s^{-1}.

Levels		$2J$						
i	k	i	k	λ (Å)	S	f	A_{ki} (s^{-1})	δT
$4p^6 4d - 4p^5 4d^2(_2{}^3F)$								
^2D	$^4D^o$	5	3	93.710	6.217×10^{-5}	2.015×10^{-4}	3.827×10^{7}	0.333
^2D	$^4F^o$	5	5	91.348	5.235×10^{-4}	1.741×10^{-3}	2.319×10^{8}	0.099
^2D	$^2G^o$	5	7	90.088	1.484×10^{-4}	5.003×10^{-4}	5.139×10^{7}	0.020
$4p^6 4d - 4p^5 4d^2(_2{}^3P)$								
^2D	$^4P^o$	5	3	85.897	2.013×10^{-4}	7.120×10^{-4}	1.609×10^{8}	0.113
$4p^6 4d - 4p^5 4d^2(_2{}^3F)$								
^2D	$^4D^o$	5	5	83.292	7.734×10^{-7}	2.820×10^{-6}	4.520×10^{5}	0.179
^2D	$^4F^o$	5	7	81.424	7.276×10^{-3}	2.714×10^{-2}	3.414×10^{9}	0.040
$4p^6 4d - 4p^5 4d^2(_2{}^1D)$								
^2D	$^2D^o$	5	3	80.533	1.972×10^{-3}	7.437×10^{-3}	1.912×10^{9}	0.026
$4p^6 4d - 4p^5 4d^2(_2{}^3P)$								
^2D	$^4P^o$	5	5	80.190	3.502×10^{-3}	1.327×10^{-2}	2.294×10^{9}	0.048
$4p^6 4d - 4p^5 4d^2(_2{}^1G)$								
^2D	$^2G^o$	5	7	79.053	4.708×10^{-7}	1.809×10^{-6}	2.414×10^{5}	0.585
$4p^6 4d - 4p^5 4d^2(_2{}^3P)$								
^2D	$^4D^o$	5	7	76.980	3.535×10^{-5}	1.395×10^{-4}	1.963×10^{7}	0.077
		5	5	76.694	1.825×10^{-6}	7.229×10^{-6}	1.366×10^{6}	0.994
^2D	$^4S^o$	5	3	76.242	1.817×10^{-4}	7.239×10^{-4}	2.077×10^{8}	0.025
$4p^6 4d - 4p^5 4d^2(_2{}^1G)$								
^2D	$^2F^o$	5	5	73.695	1.925×10^{-4}	7.936×10^{-4}	1.624×10^{8}	0.257
$4p^6 4d - 4p^5 4d^2(_2{}^3F)$								
^2D	$^4F^o$	5	3	71.745	1.186×10^{-3}	5.020×10^{-3}	1.626×10^{9}	0.023
$4p^6 4d - 4p^5 4d^2(_2{}^1D)$								
^2D	$^2D^o$	5	5	71.463	5.107×10^{-4}	2.171×10^{-3}	4.726×10^{8}	0.042
^2D	$^2F^o$	5	7	71.211	2.814×10^{-2}	1.200×10^{-1}	1.974×10^{10}	0.008
$4p^6 4d - 4p^5 4d^2(_2{}^3F)$								
^2D	$^2F^o$	5	7	67.075	2.820×10^{-2}	1.277×10^{-1}	2.366×10^{10}	0.013
$4p^6 4d - 4p^5 4d^2(_0{}^1S)$								
^2D	$^2P^o$	5	3	65.556	7.008×10^{-4}	3.247×10^{-3}	1.260×10^{9}	0.010
$4p^6 4d - 4p^5 4d^2(_2{}^3F)$								
^2D	$^2F^o$	5	5	63.060	3.672×10^{-1}	1.769	4.945×10^{11}	0.011
$4p^6 4d - 4p^5 4d^2(_2{}^3P)$								
^2D	$^2D^o$	5	3	62.981	3.124×10^{-1}	1.507	6.334×10^{11}	0.024
$4p^6 4d - 4p^6 4f$								
^2D	$^2F^o$	5	5	62.107	1.688×10^{-1}	8.255×10^{-1}	2.379×10^{11}	0.012
		5	7	61.628	5.272×10^{-1}	2.598	5.704×10^{11}	0.016
$4p^6 4d - 4p^5 4d^2(_2{}^3F)$								
^2D	$^4G^o$	5	5	53.622	3.718×10^{-4}	2.106×10^{-3}	8.144×10^{8}	0.018
		5	7	50.922	6.850×10^{-4}	4.086×10^{-3}	1.314×10^{9}	0.023
$4p^6 4d - 4p^5 4d^2(_2{}^3P)$								
^2D	$^2D^o$	5	5	50.725	1.989×10^{-2}	1.191×10^{-1}	5.146×10^{10}	0.011
^2D	$^4D^o$	5	3	50.489	3.644×10^{-3}	2.193×10^{-2}	1.434×10^{10}	0.031
$4p^6 4d - 4p^5 4d^2(_2{}^3F)$								
^2D	$^2D^o$	5	3	48.931	2.608×10^{-3}	1.619×10^{-2}	1.128×10^{10}	0.048
^2D	$^4D^o$	5	7	47.316	1.347×10^{-1}	8.649×10^{-1}	3.221×10^{11}	0.005
^2D	$^2D^o$	5	5	46.553	7.469×10^{-1}	4.873	2.500×10^{12}	0.004
$4p^6 4d - 4p^5 4d^2(_2{}^1D)$								
^2D	$^2P^o$	5	3	46.508	3.165×10^{-2}	2.067×10^{-1}	1.594×10^{11}	0.024
$4p^6 4d - 4p^5 4d^2(_2{}^1G)$								
^2D	$^2F^o$	5	7	46.224	7.413×10^{-1}	4.871	1.901×10^{12}	0.001
$4p^6 4d - 4p^5 4d^2(_2{}^3P)$								
^2D	$^2P^o$	5	3	46.137	4.110×10^{-1}	2.706	2.120×10^{12}	0.011
$4p^6 4d - 4p^5 4d^2(_2{}^1D)$								
^2D	$^2F^o$	5	5	46.054	1.035×10^{-3}	6.830×10^{-3}	3.580×10^{9}	0.024

TABLE VI. Comparison of present wave-function composition with ASD [19].

	Composition
(i) Energy level: 1508470 ($J = 5/2$)	
jj	$39\ 4p_-^2 4p^3 4d_-[2]4d + 27\ 4p_-^2 4p^4 4f_- + 13\ 4p_-^2 4p^3 4d_-[1]4d$
LSJ	$41\ (^1_2G)\ ^2F\ + 27\ 4p^6 4f\ ^2F + 13\ (^3_2F)^2F$
ASD	$45\ (^1_2G)\ (3/2,4) + 28\ 4p^6 4f\ (0,5/2)$
(ii) Energy level: 1542600 ($J = 3/2$)	
jj	$59\ 4p_-^2 4p^3 4d_-[3]4d$
LSJ	$32\ (^3_2F)\ ^4F + 22\ (^3_2P)\ ^2D\ + 12\ (^3_2F)\ ^2D$
ASD	$33\ (^3_2F)\ (3/2,3) + 18\ (^3_2P)\ (3/2,2)$
(iii) Energy level: 2184310 ($J = 3/2$)	
jj	$87\ 4p_- 4p^4 4d_-^2(2)$
LSJ	$44\ (^3_2F)\ ^2D + 17\ (^1_2D)^2D\ + 12\ (^3_2F)^4F$
ASD	$43\ (^1_2D)\ (1/2,2) + 28\ (^3_2P)\ (1/2,2)$

$\Delta S \neq 0$ or $\Delta L \neq 1$. Large values of δT are associated with the latter. A relative error estimate for an electric multipole (Ek) transition, is $\delta T + (2k+1)\delta E$ where δE is the relative error in the transition energy and k is the order of the multipole transition. Many $E1$ transition probabilites have $\delta T \leqslant 0.010$–0.03 or 1–3%. For $M1$ transitions, the length and velocity values are the same by definition and are not a test of the wave function. For $E2$ transitions, the Supplemental Material [17] shows that for many LS allowed $E2$ transitions, $\delta T \leqslant 0.05$–0.06 or 5–6%.

Table VIII compares the lifetimes of some levels with QR values computed from $E1$ transition rates. Generally there is excellent agreement in the two sets of results. An exception is the lifetime of the $4p^5 4d^2(^3_2F)\ ^2D^o$ level. None of these lifetimes of higher levels, are affected by $E2$, $M1$ transitions to lower odd-parity levels to the accuracy reported.

TABLE VIII. Computed lifetimes for W XXXVIII.

			Lifetimes (s)	
Label	J	Pos	This work	Theory [9]
$4p^5\ 4d^2(^3_2F)\ ^4D^o$	3/2	1	8.10×10^{-10}	8.44×10^{-10}
	1/2	1	2.54×10^{-10}	2.44×10^{-10}
$^4F^o$	3/2	5	2.16×10^{-12}	2.16×10^{-12}
$4p^5\ 4d^2(^1_2G)\ ^2F^o$	5/2	5	6.00×10^{-12}	6.50×10^{-12}
	7/2	10	5.26×10^{-13}	5.17×10^{-13}
$4p^6\ 4f\ ^2F^o$	5/2	8	1.21×10^{-12}	1.21×10^{-12}
	7/2	7	1.75×10^{-12}	1.72×10^{-12}
$4p^5\ 4d^2(^3_2F)\ ^4G^o$	5/2	9	8.90×10^{-13}	8.80×10^{-13}
$^2D^o$	3/2	9	3.11×10^{-13}	3.03×10^{-13}
	5/2	11	4.00×10^{-13}	1.02×10^{-12}

V. CONCLUSIONS

With the revised GRASP2K code, it has been possible to compute the energies of $4p^6 4d$, $4p^6 4f$, and $4p^5 4d^2$ levels and all $E1$, $E2$, and $M1$ transitions between them to high accuracy using the SD-MR method. Because the $4d$ and $4f$ subshells of the $n = 4$ shell are unfilled, the interaction with other configurations from the $n = 4$ complex are of prime importance. The major components of the wave function have been compared in both jj and LSJ coupling. Although in jj coupling most of the expansions have a dominant component, the LSJ label can be used to identify the LS-forbidden transitions. The property of being LS forbidden explains the larger error estimates for such a transition. Finally, we estimated the lifetime of $4p^6 4d\ ^2D_{5/2}$ to be 25.2(2) ms.

ACKNOWLEDGMENTS

G. Gaigalas is grateful to the Atomic Spectroscopy Group at the National Institute of Standards and Technology for hospitality and support during his visit.

TABLE VII. Comparison of computed wavelengths from different theories with observed wavelengths for transitions from $4p^6 4d\ ^2D$ to selected upper levels.

Upper	$2J_i$	$2J_k$	QR [9]	PP [3]	Expt. [2]	This work
$4p^6 4d\ ^2D$	3	5			646.7(5)[a]	647.86
$4p^5\ 4d^2(^3_2F)\ ^2D^o$	3	3	45.312	44.766	45.7810(22)	45.495
$4p^5\ 4d^2(^3_2P)\ ^2P^o$	5	3		45.480	46.0640(55)	46.137
$4p^5\ 4d^2(^1_2G)\ ^2F^o$	5	7	46.007	45.556	46.0640(55)	46.224
$4p^5\ 4d^2(^3_2F)\ ^4G^o$	3	5	49.215	49.030	49.6407(54)	49.523
$4p^6\ 4f\ ^2F^o$	3	5	56.332	56.055	56.8797(41)	56.674
$4p^5\ 4d^2(^3_2F)\ ^2F^o$	3	5	57.029	56.680	57.7547(14)	57.467
$4p^6\ 4f\ ^2F^o$	5	7	61.158	60.922	61.9200(83)	61.628
$4p^6\ 4f\ ^2F^o$	5	5		61.340	61.9200(83)	62.107
$4p^5\ 4d^2(^3_2F)\ ^2F^o$	5	5		62.090	63.4319(119)	63.060
$4p^5\ 4d^2(^3_2P)\ ^2D^o$	5	3		62.138	63.4319(119)	62.981
$4p^5\ 4d^2(^3_2F)\ ^4F^o$	3	3	64.029	63.775	64.8250(200)	64.592
$4p^5\ 4d^2(^1_2G)\ ^2F^o$	3	5	65.703	65.703	66.29 252(147)	66.169
$4p^5\ 4d^2(^3_2F)\ ^4D^o$	3	1	81.222	81.299	81.4573(89)	81.841
$4p^5\ 4d^2(^3_2F)\ ^4D^o$	3	3	81.228	81.359	81.4573(89)	81.868

[a]From Radtke *et al.* [7].

[1] G. Gaigalas, Z. Rudzikas, E. Gaidamauskas, P. Rynkun, and A. Alkauskas, Phys. Rev. A **82**, 014502 (2010).
[2] S. B. Utter, P. Beiersdorfer, and E. Träbert, Can. J. Phys. **80**, 1503 (2002).
[3] K. B. Fournier, At. Data Nucl. Data Tables **68**, 1 (1998).
[4] M. Klapisch, Comput. Phys. Commun. **2**, 239 (1971).
[5] M. Klapisch, J. L. Schwob, B. Fraenkel, and J. Oreg, J. Opt. Soc. Am. **67**, 146 (1977).
[6] A. E. Kramida and T. Shirai, At. Data Nucl. Data Tables **95**, 305 (2009).
[7] R. Radtke, C. Biedermann, J.-L. Schwob, P. Mandelbaum, and R. Doron, Phys. Rev. A **64**, 012720 (2001).
[8] R. D. Cowan, *The Theory of Atomic Structure and Spectra* (University of California Press, Berkeley, 1981).
[9] P. Bogdanovich and O. Rancova, A. Štikonas Phys. Scr. **83**, 065302 (2011).
[10] P. Jönsson, X. He, C. Froese Fischer, and I. P. Grant, Comput. Phys. Commun. **177**, 597 (2007).
[11] P. Jönsson, G. Gaigalas, J. Bieroń, C. Froese Fischer, and I. P. Grant (unpublished).
[12] G. A. Gaigalas, Z. B. Rudzikas, and C. Froese Fischer, J. Phys. B **30**, 3747 (1997).
[13] Z. Rudzikas, *Theoretical Atomic Spectroscopy*, 2nd ed. (Cambridge University Press, Cambridge, 2007).
[14] I. P. Grant, *Relativistic Quantum Theory of Atoms and Molecules* (Springer, New York, 2007).
[15] B. J. McKenzie, I. P. Grant, and P. H. Norrington, Comput. Phys. Commun. **233**, 597 (1980).
[16] C. Froese Fischer, J. Phys. B **44**, 125001 (2011).
[17] See Supplemental Material at http://link.aps.org/supplemental/10.1103/PhysRevA.85.042501 for a table of MCDHF $E2$ and $M1$ transition data for transitions between all levels. Included are the wavelength, line strength, f value, and transition probability for each transition and the δT for all $E2$ transitions.
[18] C. Froese Fischer and G. Tachiev, MCHF/MCDHF Database [http://physics.nist.gov/mchf] (2011).
[19] Yu. Ralchenko *et al.*, NIST Atomic Spectra Database [http://physics.nist.gov/asd] (2011).
[20] C. Froese Fischer and G. Tachiev, At. Data Nucl. Data Tables **87**, 1 (2004).
[21] C. Froese Fischer, J. Phys. B **43**, 074020 (2010).